

Design of Elastic Component of Optic Intensity Force Sensing Catheter Based on Finite Element Analysis

Yun Zou^{1,2}, Hao Liu², *Member, IEEE*, Anzhu Gao², *Student Member, IEEE*, Yuanyuan Zhou², Siwen Hao²

1. Department of Mechanical Engineering, Shenyang Ligong University, Shenyang 110159, China

2. State Key Laboratory of Robotics, Shenyang Institute of Automation, Chinese Academy of Sciences, Shenyang 110016, China
E-mail: liuhao@sia.cn

Abstract: This paper presents a design method of a miniaturized force sensing elastic component for the cardiac catheter. It is used to sense the contact force between the interaction of the catheter tip and surrounding tissue. A spring-like elastic structure was designed to accomplish its function. The method based on the finite element analysis (FEA) was proposed to help design the spring-like structure. The experiment was carried out to calibrate the material property and verify its feasibility. Simulations with variable spring parameters were done to investigate the effects of the stiffness to the micro deformation. Results indicate that the proposed structure can provide a good force sensing capability.

Key Words: Elastic component, Force sensing catheter, Finite element analysis, Cardiac surgery

1. INTRODUCTION

Minimally invasive surgery (MIS) is popular with its smaller skin incision, fewer pains, and less blood loss when compared with the open surgery. However, a conventional catheter would lead to poor maneuverability and disoperation with a defined distal shape [1]. Because an inconvenience long ablation catheter, lacks of depth and haptic information, restricting surgeon's movement, MIS produce lengthening of the operation time and incompleteness of operation result [2]. The catheter exerts forces on blood vessel walls at its tip and sides when it moves inside a patient's vasculature system. If a catheter is inserted manually, these forces at the end of the catheter can be sensed as haptic feedback through doctors' hands. Therefore, since excessive forces can tear blood vessels or tissue would hurt patients and cause damages, the procedure requires skilled and experienced surgeons are required to insert the catheter during the procedure [3]. But a precision about 2mm can be achieved by an experienced doctor in the surgery. They cannot sense the contact force between the blood vessel and the catheter, and confront dangers of mingling or breaking the blood vessels [4]. To solve these problems, more and more miniaturized force sensors are designed.

¹Recently, many different force sensing methods were proposed. For example, polyvinylidene fluoride (PVDF) films were used as the tactile sensor in the catheter side wall for MIS [5], a micro touch sensor was developed by utilizing PZT (lead zirconate titanate) as piezoelectric material [6], piezoresistivity was used in the sensory system with intravascular navigation [7], M. Tanimoto has fabricated a micro sensor for intravascular neurosurgery [8], the uniaxial and multi-axes force

sensors were used to acquire contact forces during MIS [9] and particular forces from a catheter inside a heart [10]–[12], strain gauges [13], and fiber optic technology [14][15]. The catheter-tip and sidewall miniature pressure sensors based on silicon-diaphragm have been developed [16]. To provide the sufficient information of the catheter tip–tissue interaction forces from haptic feedback. Many different types of sensors are developed and integrated with medical catheters. However, they focused on the design of the different types of force sensing solution, which takes the critical role to produce the enough axial and lateral elasticity, in order that the solution based on optical intensity [17] can measure its deformation with high accuracy within the yielding stress of material.

We developed the force sensing solution using the spring-like structure [17] to provide the good force prediction. In this paper, we propose a solution based on the FEA to help design the structure in order to improve the function of the elastic component. In Section II, we introduced the force sensing solution and the design of the miniature elastic component. Section III introduced the solution based on FEA to simulate the deformation of elastic structure. Section IV carried out the experiment to calibrate the material property and compared its results with the simulation. Section V discussed the effects of variable spring parameters. Section VI concluded the paper.

2. THE FORCE SENSING SOLUTION BASED ON OPTICAL INTENSITY

2.1 The Principle of Intensity Based Force Sensing Catheter

For the principle of light intensity sensor, it has been used for many aspects. A primary principle is modulation of light. A fiber-optic sensor contains three main parts: the optical detector, the light modulator element and the light source [3]. The light source makes

This work is supported by National Nature Science Foundation under Grant No.61473281 and No.61503370, and The Doctoral Scientific Research Foundation under Grant No.20141151.

the light, through the optical transmitting fiber the light modulator element. When a force is applied at the tip of the catheter, the fiber-optic detector is based on light intensity modulation caused by the change of the reflector [18]. Then the light is transformed to an electrical signal and it is amplified. The voltage output can be transformed to the force.

2.2 Design Standard of Force Sensor

The different advantages of a force sensor adapt the envisaged application area. Accordingly, the specifications for a cardiac catheter force sensor need be identified. And the size of the force sensor is quite important advantage. The size changes along with the change of its elastic component. That affects the measuring performance of a catheter force sensor. In order to fit inside blood vessels in MIS, a sensor should have a small diameter of around 6–15Fr (2–4.5mm), and it is the same as a small diameter of cardiac catheters. The other small diameter of a miniaturized catheter needs to become an important factor when developing a cardiac catheter force sensor [19]. To avoid some complex miniaturization issues, force sensors are applied to arrangements attached outside, but near the patients. The force sensors use the catheter shaft as the force/torque transmission element [20]. The length of force sensors needs to be determined according to the application background. This paper is in view of the minimally invasive vascular surgery, its length should not be too large, otherwise that will affect the blood vessel and measurement accuracy, we set the length is 10mm.

The ability to detect forces of a specific range with high sensitivity and resolution is the other advantage of a cardiac catheter force sensor. The suitable contact force required to achieve a safe ablation line in RF procedures is around 0.2-0.3N of force, that is identified by interventional cardiologists [21]. However, these sensors are expected to support higher forces (~1–3N) when the catheter is passing through the hemostatic sheaths that keep the blood arteries open [22]. Therefore, when exposed to forces exceeding 1 N, the design should ensure that the elastic component will not be damaged.

2.3 Miniaturized Force Feedback Elastic component Design

According to the requirement of the sensor design, design of miniaturized force feedback elastic component adapts to the same specification. The structure of the proposed force sensor in this paper mainly has four parts: a) the catheter tip; b) the force-deformation transferring part (the miniaturized force feedback elastic component); c) the optical fibers; d) the fibers alignment module. The linear deformation of b) can be beneficial to the accuracy of measurement of the sensor. The part a) can provide a reflective surface. The part d) contains a 0.25-mm-diameter optical fiber that allows measurement

of the magnitude of the catheter contact force. The elastic deformation of b) is used to transform the distal force measuring to the reflective surface's displacement detection by exerted a load.

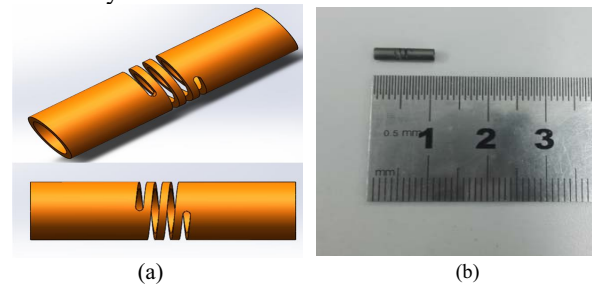


Fig. 1. Photo of the elastic component design model and the part

The structure of the elastic component is designed to be similar to the spring; we can take full advantage of its bending properties. Figure 1 a) shows the design model. The structure can be rectangular or cylindrical tube shape, and we select tube type in order to adapt to surgical medical catheter sensor. A maximum external diameter of the assembled sensor parts is 7Fr (2.34mm) and the length is 17mm. Get rid of the connectors, we design the length is 10mm. Then we confirm the length of the elastic component, the pitch of the spring and width of wire will be principal factors. We design the maximum external diameter is 2.6mm. A processed part is illustrated in Figure 1 b). Sensor should be set on a catheter shaft, and a lumen in the center of the elastic component must be provided to permit a space for electrode leads or other equipment, a diameter of 2mm. Due to the material of elastic component also affects the measuring performance of a catheter force sensor. In order to make use of better material properties, we choose TC4 (Ti-6Al-4V) which has the good comprehensive mechanical properties. For the structure, we design a thread pitch is 0.6 mm and a slot width is 0.3 mm. A photograph of the integrated prototype elastic component is illustrated in Figure 2.



Fig. 2. The integrated prototype elastic component

3. METHOD BASED ON FEA

For the elastic component configuration which is similar to the spring structure. ABAQUS (finite element analysis software) is used to research the behavior, achieve some parameters of force, and make sure the elastic component within the specified working ranges. Here we use the Abaqus 6.13 (Simulia, USA) to simulate

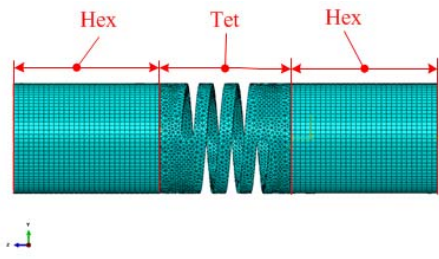


Fig. 3. The distribution of mesh controls

the deformation of the elastic component. The procedure of simulation is introduced below.

Step1: Material property

According to the later comparison of methods, we set Young's modulus is 130GPa and Poisson's ratio is 0.34 in step of material property.

Step2: Boundary Condition

We choose the underside of elastic component as factor in step of boundary condition, in this way, the axial and lateral force simulation can be received.

Step3: Load

Due to the requirements for our force sensor [17], the flexure should be able to measure a maximum force of up to 1N (~100 gm of force). In step of load, we set the load is 1N.

Step4: Mesh

Mesh is the important setting part of Abaqus 6.13, that is affected the quality of simulation greatly. In Figure 3, model of the elastic component is divided in three parts. We set tetrahedron (Tet) and hexahedron (Hex) in different section in the model. The middle section is the grooving part of it and that was set Tet, sufficient simulation will be done.

Step5: Analysis Type

Static analysis was set to be static analysis. Nonlinear option was chose to simulate the large deformation.

Step6: Job

According to the above steps, the simulations would be calculated in job.

4. EXPERIMENTAL AND SIMULATION RESULTS

4.1 Experimental Setup

In order to verify these simulation results, as shown in Figure 4, we build experimental platform which contains the miniaturized force feedback elastic component, the force sensor, the DAQ card, the adjustable power supply, the desktop computer and the linear motor. The type of the force sensor is FUTEK LSB 200, it has a working range of 1 lb. The accuracy of measurement is 1% of full scale. We can achieve the miniaturized force feedback elastic component is linearly deformed when exerted axial loads up to 1N from the results of simulation. The model of the DAQ

card is USB-6221 of National Instruments; its sample rate can be 250Ks/s. The linear motor is LMCB5, made by HIWIN, its mass of force is 0.48Kg and minimum step distance is 0.001mm.

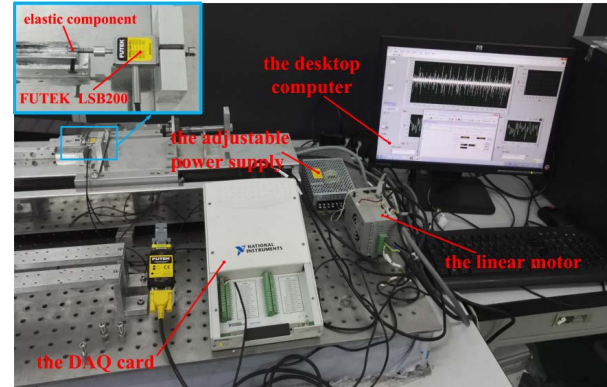


Fig. 4. The experiment equipment platform

First, the linear motor drives the FUTEK sensor to approach the elastic component or elastic part tip (the tip of miniaturized force feedback elastic component which is manufactured). Before the experiments, we need make the distance from the FUTEK sensor to the flexible part tip is adjusted to the position where the FUTEK sensors stick to the tip while exerted on no load. When they begin to contact, an axial load is exerting on the flexible part. We set the forward distance of the linear motor is 0.002mm as same as the FUTEK sensor. Then the slider of linear motor will be driven left to increase the deformation of the flexible part. Obtaining and recording the data of the contacted force as the sensor advance very time on the computer. Until the data of the contacted force is quite close to 1N, we adjust motor direction of the linear motor by the same rules. At the same time, the displacement of the linear motor will be recorded.

4.2 Calibration of Material Property

Material property, especially the Young's modulus varies according the manufacture process. So we carried out an experiment to calibrate the Young's modulus.

The material of elastic component we choose is TC4 (Ti-6Al-4V), its theoretical parameters are used in Abaqus 6.13 of this paper and they should approach the actual argument of elastic component which we designed. There are two primary parameters, Young's modulus and Poisson's ratio. The Poisson's ratio is 0.34. In fact, Young's modulus of this actual elastic component may not be the theoretical value we often use, so we must confirm the proper parameter. First, the theoretical Young's modulus is 113GPa, that is used in ABAQUS and we get relational data of the axial displacement and the corresponding force. By comparing these with the data of the experiment and modifying the appropriate parameter appropriately, then we carry on the simulation again. Through several

modifications and simulations, the range of parameter determination is narrowed down.

Compare the relationship between force and shape change with the relationship from above simulation, we can get relatively accurate material property, include the Young's modulus. The last Young's modulus is 130GPa and it is optimal parameter of our elastic component.

4.3 Comparison of Results

Due to the elastic component is the key part of this force sensor, its design plays an important role on the force sensor performance. When the miniaturized force feedback elastic component is under the action of external force, there is a relation between its deformation and the force. In addition, the structure of the elastic component should be small enough to integrate with catheters; it should be good for sensitivity of sensor and favor the catheter in the space within the flexible movement. When the forces are acting on the tip of the catheter, that has an obvious impact on the horizontal beams causing them to deform.

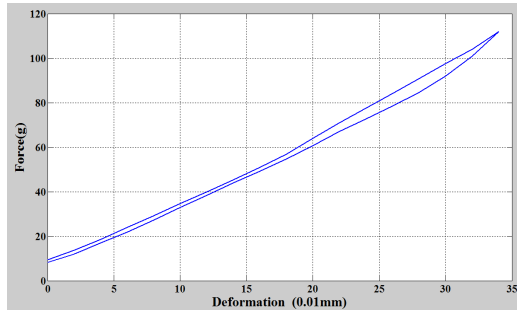


Fig. 5. The experimental data from the analysis of the elastic component

The data of experimental results transform between the deformations of the force is shown in Figure 5. We choose axial loading experiment as example. We can get the rule between deformation and force loaded to nearly 1N. It can be inferred that there exists quite good linearity between the deformation and the force. The configuration and size of miniaturized force feedback elastic component are relatively rational.

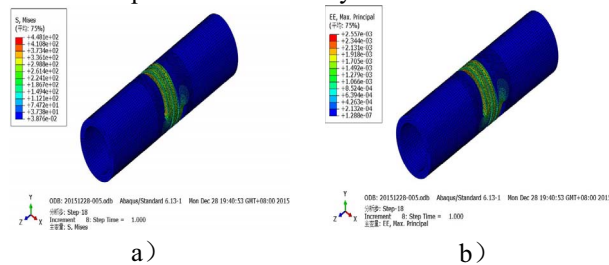


Fig. 6. Stress distribution and elastic deformation of different elastic components under an axial load of 1N

Figure 6 a) and b) are the simulation results of the elastic component. Von-Mises stress and the principal elastic deformation can be obtained from them. Its maximum Von-Mises stress is 448.1MPa and maximum elastic deformation is 2.557×10^{-3} mm. Theoretical Yield Strength of TC4 is under 860MPa, the elastic component

we designed is coincident. The curve from experiment tallied closely with the curve from simulation model, which has confirmed the accuracy of the method.

5. DISCUSSION

5.1 Simulation of the elastic structure with lateral force

Except the axial force simulation, we also consider the lateral tip loading conditions (1N), the steps in ABAQUS are the same as a axial load of 1N except the direction of applied load. Its simulation can be saw in Figure 7. The maximum Von-Mises stress is 333.3MPa and maximum elastic deformation is 2.400×10^{-3} mm, which is bigger than the axial load. Data of lateral load of the elastic component we designed is coincident to Yield Strength of TC4.

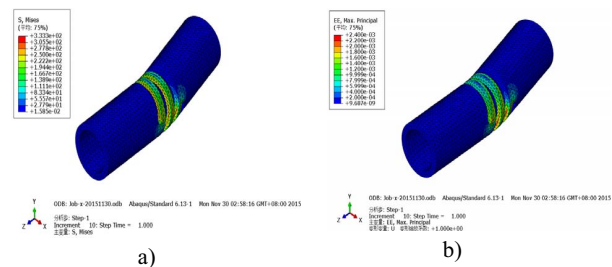


Fig. 7. Stress distribution and elastic deformation of our elastic component under a lateral load of 1N

5.2 Simulation of the elastic structure with variable flexure

We make the analysis of condition by this structure condition with different size to verify rationalization of the proposed configuration. Because we confirm the length of the elastic component, the pitch of the spring and width of wire is the principal factors of the structure.

We propose different size of the pitch and width of wire and use ABAQUS to research the behavior and elastic deformation (Figure 8), the elastic deformation of different elastic components is under a axial load of 1N. By contrast with the elastic component we designed (the pitch of the spring is 0.6mm and width of wire is 0.3mm), Figure 5 a) and b) show the same pitch of the spring is 0.6mm, width of wire are 0.2mm and 0.4mm, the former max elastic deformation is 1.718×10^{-3} mm and the latter is 4.722×10^{-3} mm. We can obtain the elastic deformation of the elastic component we designed is between them. Figure 5 c) and d) show the same width of wire is 0.3mm, he same pitch of the spring are 0.5mm and 0.7mm, the former max elastic deformation of the former is 4.916×10^{-3} mm and the latter is 1.702×10^{-3} mm. The elastic deformation of the elastic component we designed is also between them. That indicates size of the pitch and width of wire are changed, the elastic deformation change up and down.

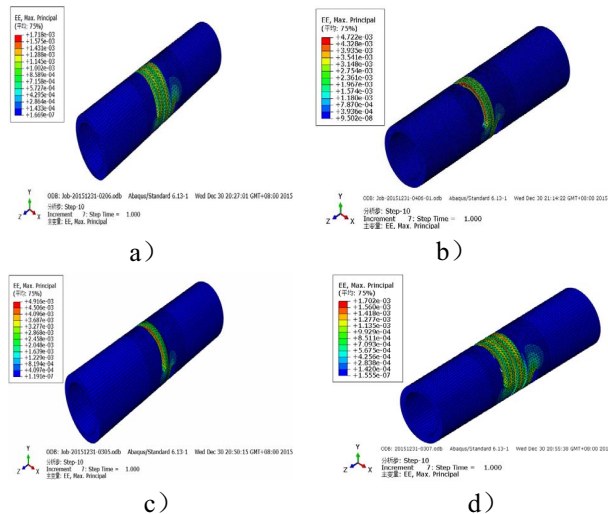


Fig. 8. Elastic deformation of different elastic components under a axial load of 1N

Data from the above simulations of different size of the pitch and width of wire can be achieved, they are imported in Matlab and the relation between deformation and the force under a axial load of 1N is saw in Figure 9. As shown in the figure, when the same pitch of spring is 0.6mm, the red line (A1) represents the relation of deformation and the force as the width of wire is 0.2mm, the green line (A2) represents the width of wire is 0.4mm. When the same width of wire is 0.3mm, the blue line (B1) represents the relation of deformation and the force as the pitch of spring is 0.5mm, the black line (B2) represents the pitch of spring is 0.7mm. We can find the data demonstrate quite good linearity between the deformation and the force. A1 and A2 show that the tendency of elastic deformation has large difference in the same pitch of spring and different width of wire. Similarly, B1 and B2 show that the tendency of elastic deformation has large difference in the same width of wire and different pitch of spring. But A1 and B2, the two kinds of different size of simulation model have the quite close tendency of elastic deformation. The close tendency can also be found in A2 and B1. We can find some relations between the elastic deformation and the elastic structure.

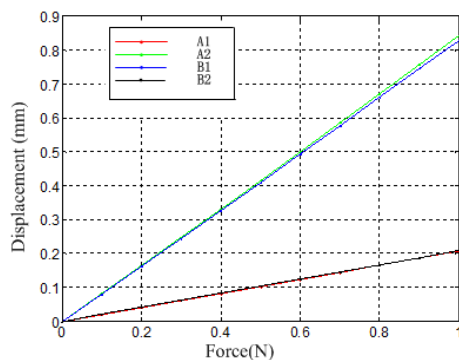


Fig. 9. Relation between deformation and the force of different sizes under a axial load of 1N

6. CONCLUSION

Optic intensity force sensing catheter was developed and integrated to assist the cardiac surgeon with real-time and precise force feedback in this paper. The usage of reasonable material, the optimal structural design of the elastic component, and the application of optic intensity force sensing catheter greatly promise an accurate force sensor. The simulation and experimental results indicate that the miniaturized force feedback elastic component can work with fairly good linearity. It has the potential to be used in optic intensity force sensing catheter of MIS.

In the future, we will continue to design a parameter-optimized elastic component used for 3D force sensing solution.

REFERENCES

- [1] Yili Fu, Anzhu Gao, Hao Liu, et al, Development of a Novel Robotic Catheter System for Endovascular Minimally Invasive Surgery, IEEE/ICME International Conference on Complex Medical Engineering,400-405, 2011.
- [2] Ho Seok Song, Ju Won Jeong, Jung Ju Lee, Optical fiber Bragg grating (FBG) force reflection sensing system of surgical tool for minimally invasive surgery, IEEE 9th Conference on Industrial Electronics and Applications (ICIEA),478-482, 2014.
- [3] Panagiotis Polygerinos, Dinusha Zbyszewski, Tobias Schaeffter, et al, MRI-Compatible Fiber-Optic Force Sensors for Catheterization Procedures IEEE International Conference on Systems, IEEE SENSORS JOURNAL, VOL. 10, NO. 10,1598-1608,2010.
- [4] Xu Ma, Shuxiang Guo, Shuxiang Guo, et al, Development of a Novel Robot-Assisted Catheter System with Force Feedback, IEEE International Conference on Mechatronics and Automation ,107- 111, 2011.
- [5] F. WeiXing, W. HuanRan, G. ShuXiang, W. KeJun, and Y. XiuFen, "Design and experiments of a catheter side wall tactile sensor for minimum invasive surgery", Int. Conf. on Mechatronics and Automation, Harbin, pp.1073-1078,2007.
- [6] L. Du, H. Zhao, F. Toshio, F. Arai, "Micro touch sensor using piezoelectric thin film for minimal access surgery", Chinese journal of mechanical engineering, vol 18, pp.87-91, No.1, 2005.
- [7] D. Tanase, J. F. L. Goosen, P. J. Trimp, and P. J. French, "Multi-parameter sensor system with intravascular navigation for catheter/guide wire application," Sens. Actuators A, pp. 116-124, 2002.
- [8] M. Tanimoto, F.Arai, T. Fukuda, H. Iwata, K. Itoigawa, Y. Gotoh, M. Hashimoto, M. Negoro, "Micro force sensor for intravascular neurosurgery and in vivo experiment", The Eleventh Annual International Workshop on Micro Electro Mechanical Systems, 1998. MEMS 98. Proceedings, pp.504 - 509, Jan. 1998.
- [9] P. Puangmali, H. Liu, L. D. Seneviratne, P. Dasgupta, and K. Althofer, "Miniature 3-axis distal force sensor for minimally invasive surgical palpation," IEEE/ASME Trans. Mechatronics, [Online]. Available: <http://ieeexplore.ieee.org>, DOI: 10.1109/TMECH.2011.2116033.

- [10] M. C. Yip, S. G. Yuen, and R. D. Howe, "A robust uniaxial force sensor for minimally invasive surgery," *IEEE Trans. Biomed. Eng.*, vol. 57, no. 5, pp. 1008–1011, Feb. 2010.
- [11] S. B. Kesner and R. D. Howe, "Design and control of motion compensation cardiac catheters," in *Proc. IEEE Int. Conf. Robot. Autom.*, Anchorage, AK, 2010, pp. 1059–1065.
- [12] S. B. Kesner and R. D. Howe, "Design principles for rapid prototyping force sensors using 3D printing," *IEEE/ASME Trans. Mechatronics*, vol. 16, no. 5, pp. 866–870, Oct. 2011.
- [13] H. Allen, K. Ramzan, J. Knutti, and S. Withers, "A novel ultra-miniature catheter tip pressure sensor fabricated using silicon and glass thinning techniques," in *Proc. Materials Research Soc. Conf.*, San Francisco, CA, 2001, p. 17.4.
- [14] C. Strandman, L. Smith, L. Tenerz, and B. Hok, "A production process of silicon sensor elements for a fibre-optic pressure sensor," *Sens. Actuators A*, vol. 63, no. 1, pp. 69–74, 1997.
- [15] E. Cibula, D. Donagic, and C. Stropnik, "Miniature fiber optic pressure sensor for medical applications," in *Proc. IEEE Sens.*, 2002, pp. 711–714.
- [16] M. Esashi, H. Komatsu, T. Matsuo, M. Takahashi, T. Takishima, K. Imabayashi, H. Ozawa, "Fabrication of catheter-tip and sidewall miniature pressure sensors," *IEEE transactions on electron devices*, vol. ED-29, pp.57-63, Jan 1982.
- [17] Zhenda Yang, Hao Liu, Yuanyuan Zhou, et al, "A miniature force sensor for catheter based on optical micro deformation detection", *IEEE International Conference on Cyber Technology in Automation, Control, and Intelligent Systems (CYBER)*, IEEE, 441 – 445, 2015.
- [18] Panagiotis Polygerinos, Tobias Schaeffter, Lakmal Seneviratne, et al, "A Fibre-Optic Catheter-Tip Force Sensor with MRI Compatibility: A Feasibility Study," *IEEE International Conference on Mechatronics and Automation Annual International Conference of the IEEE EMBS Minneapolis*, 1501- 1504, 2009.
- [19] P. Polygerinos, D. Zbyszewski, T. Schaeffter, R. Razavi, L. D. Seneviratne, and K. Althoefer, "MRI-compatible fiber-optic force sensors for catheterization procedures," *IEEE Sens. J.*, vol. 10, no. 10, pp. 1598–1608, Oct. 2010.
- [20] P. Kanagaratnam, M. Koa-Wing, D. T. Wallace, A. S. Goldenberg, N.S. Peters, and D. W. Davies, "Experience of robotic catheter ablation in humans using a novel remotely steerable catheter sheath," *J. Interv. Card. Electrophysiol.*, vol. 21, no. 1, pp. 19–26, 2008.
- [21] K. Yokoyama, H. Nakagawa, D. C. Shah, et al, "Novel contact force sensor incorporated in irrigated radiofrequency ablation catheter predicts lesion size and incidence of steam pop and thrombus," *Circulation*, vol. 1, no. 5, pp. 354–362, 2008.
- [22] Panagiotis Polygerinos, Lakmal D. Seneviratne, Reza Razavi, et al, "Triaxial Catheter-Tip Force Sensor for MRI-Guided Cardiac Procedures," *IEEE Trans. on Automatic Control*, Vol.50, No.4, 511-515, 2005.